Static and dynamic polar nanoregions in relaxor ferroelectric Ba(Ti$_{1-x}$Sn$_x$)O$_3$ system at high temperature

L. Xie,[1,2] Y. L. Li,[1,2] R. Yu,[1,2] Z. Y. Cheng,[1,2] X. Y. Wei,[3] X. Yao,[3] C. L. Jia,[3,4] K. Urban,[4] A. A. Bokov,[5] Z.-G. Ye,[3,5] and J. Zhu[1,2,*]

[1]*Beijing National Center for Electron Microscopy, Tsinghua University, Beijing 100084, China*

[2]*Department of Materials Science and Engineering, the State Key Laboratory of New Ceramics and Fine Processing, Laboratory of Advanced Materials, Tsinghua University, Beijing 100084, China*

[3]*Electronic Materials Research Laboratory, Key Laboratory of the Ministry of Education and International Center for Dielectric Research, Xi'an Jiaotong University, Xi'an 710049, China*

[4]*Peter Grünberg Institute and Ernst Ruska Center for Microscopy and Spectroscopy with Electrons, Forschungszentrum Jülich, D-52425 Jülich, Germany*

[5]*Department of Chemistry and 4D LABS, Simon Fraser University, Burnaby, British Columbia V5A 1A6, Canada*

(Received 3 November 2011; revised manuscript received 17 December 2011; published 30 January 2012)

Relaxor ferroelectrics are materials exhibiting dielectric dispersions in their maximum permittivity temperature without macroscopic phase transition into a ferroelectric state. Their exceptional properties are exploited in a variety of dielectric and piezoelectric applications. As it is generally believed that polar nanoregions play a crucial role in relaxor behavior, there are great interests in exploring how the atomic structures affect the relaxor properties. Here, using the dark field imaging and atomic-resolution electron microscopy, we investigate the nano and atomic structure of a lead-free ferroelectric-relaxor Ba(Ti$_{1-x}$Sn$_x$)O$_3$ system at high temperature. The local atom displacements and their spatial correlations are measured, and the atomic structure of static polar nanoregions in the relaxors is reported. For the materials exhibiting normal ferroelectricity, no such static polar structures can be seen. Based on our experimental observations, we suggest the static polar nanoregions are responsible for the relaxor behavior in this lead-free system.

PACS number(s): 77.22.Gm, 77.80.Jk, 68.37.Og

I. INTRODUCTION

Relaxor ferroelectrics (relaxors for short) are characterized by a broad maximum of their dielectric permittivity and by a pronounced frequency dependence of T_m, the temperature of permittivity maximum. Owing to their fascinating properties, relaxors with complex perovskite structure, such as Pb(Mg$_{1/3}$Nb$_{2/3}$)O$_3$ (abbreviated by PMN) and Pb(Zn$_{1/3}$Nb$_{2/3}$)O$_3$, have been widely used as high-permittivity tunable dielectrics[1] and electrostrictive and piezoelectric actuators and sensors.[1,2] However, considering the possible harm to the environment, lead-containing materials are highly undesirable, and research interest in the lead-free materials as a substitute has been revived.[3–5] In particular, BaTiO$_3$-based relaxors, such as Ba(Ti$_{1-x}$Sn$_x$)O$_3$ (BTSn) and Ba(Ti$_{1-x}$Zr$_x$)O$_3$, are widely studied.[3–10]

It is now generally believed that polar regions of nanometer size play an important role in relaxor behavior for both lead-containing and lead-free relaxor materials.[11,12] The polar nanoregions can either result from structural disorder or chemical disorder. For lead-based relaxors, it was suggested that the chemically ordered regions[13–16] or the random distribution of B-site atoms[17–19] constitute the necessary condition for the appearance of polar nanoregions. The chemically ordered regions either act as sites to localize the polar nano-regions (PNRS) in a dynamic way[16] or as sites to pin the PNRs in a static way.[20] Using the neutron elastic diffuse scattering,[21] it was shown that both the size of the PNRs and the integrated diffuse intensity increase with cooling. For lead-free relaxors, however, the relation between the PNRs, the structural disorder, and the relaxor behavior are still poorly understood and in controversy. For instance, using electron diffraction, it was shown that

the diffuse scatterings in BaTiO$_3$-based relaxors, which are the main character of polar structures, remain essentially identical for compositions ranging from ferroelectrics to relaxors irrespective of the structure.[9,22] This suggests that the correlation length of PNRs is almost unchanged in both the ferroelectrics and the relaxors.[23] In contrast, a complex domain structure with an average domain size of 100×100 nm^2 in the ferroelectric BTSn was reported by using the piezoresponse force microscopy,[24] but no piezoactivity could be found in the relaxor BTSn.[24]

To fully understand the PNRs, structural disorder, and their relation to the relaxor behavior in the lead-free relaxors, we carried out structure characterizations of Ba(Ti$_{1-x}$Sn$_x$)O$_3$ at ambient temperature by means of conventional dark field imaging and aberration-corrected high-resolution transmission electron microscopy. Combining these techniques, we investigate the nanoscale information as well as the atomic details of the PNRs in both ferroelectric and relaxor compounds (see the Methods section and Supplemental Material[25]).

II. METHOD

The Ba(Ti$_{1-x}$Sn$_x$)O$_3$ ceramics were synthesized by conventional solid-state reactions.[10] The crossover from the ferroelectric state to the relaxor state at a composition $x = 0.19$ was determined from the dielectric measurement.[3,10] A detailed dielectric phase diagram can be found in Ref. 3. The specimens for transmission electron microscopy were prepared by standard procedures, including grinding, dimpling, and polishing, followed by a final thinning performed by Ar ion milling in a stage cooled by liquid nitrogen. Dark

field images were recorded on a conventional FEI Tecnai G2 microscope operated at 200 kV. High-resolution transmission electron microscopy investigations were performed on an FEI Titan 80-300 electron microscope with the image aberration corrector. The negative C_S imaging (NCSI)[26–28] technique was employed in our experiments to investigate the atomic structure of PNRs. Before image recording, the lens aberrations, e.g. spherical aberration, twofold, threefold astigmatism, and coma of the objective lens were measured by evaluating the Zemlin tableaus. According to the measurements, the spherical aberration is -13 μm with twofold astigmatism, threefold astigmatism, and coma minimized to obtain the highest resolution. Images were recorded on a Gatan 2 × 2-k CCD camera at a sampling rate of about 0.0094 nm per pixel. Structure modeling and image simulations were carried out using the MacTempasX software package.[29]

III. RESULTS AND DISCUSSIONS

The experiment was conducted for three compositions Ba(Ti$_{0.84}$Sn$_{0.16}$)O$_3$, Ba(Ti$_{0.8}$Sn$_{0.2}$)O$_3$, and Ba(Ti$_{0.75}$Sn$_{0.25}$)O$_3$. According to the dielectric phase diagram,[3] Ba(Ti$_{0.84}$Sn$_{0.16}$)O$_3$ is a ferroelectric material, while Ba(Ti$_{0.8}$Sn$_{0.2}$)O$_3$ and Ba(Ti$_{0.75}$Sn$_{0.25}$)O$_3$ are relaxors. The temperatures of the dielectric peak maximum (T_m) for these three materials are 275, 240, and 200 K, respectively. The freezing temperatures (T_f) for the relaxors are about 240 and 180 K. Therefore, our room-temperature investigations were well above the freezing temperature T_f of polar nanoregions for the relaxor compounds, i.e. the materials are in the ergodic relaxor phase.[3,30] The polar structures of Ba(Ti$_{1-x}$Sn$_x$)O$_3$ are characterized by {100}* diffuse sheets in reciprocal space, and we employed these diffuse intensities for dark field imaging (see the Supplemental Material[25]). Figure 1 shows the dark field images of (a) Ba(Ti$_{0.8}$Sn$_{0.2}$)O$_3$, (b) Ba(Ti$_{0.75}$Sn$_{0.25}$)O$_3$, and (c) Ba(Ti$_{0.84}$Sn$_{0.16}$)O$_3$ with their electron diffraction patterns displayed in the insets, respectively. The white circles in the electron diffractions denote the diffuse scatterings used for imaging. The dark field images clearly demonstrate the structural difference between the relaxor compounds and the ferroelectric compound and, as are displayed in Figs. 1(a) and 1(b), the relaxors Ba(Ti$_{0.8}$Sn$_{0.2}$)O$_3$ and Ba(Ti$_{0.75}$Sn$_{0.25}$)O$_3$ are characterized by a grey uniform intensity background as well as superimposed distinct, sharp, and very bright polar regions. The size of these bright regions ranges from subnanometers to a few nanometers. Moreover, it should be noted that these bright polar regions are quite stable since their shape and size remains almost unchanged during the acquisition of the dark field images. On the contrary, the image of Ba(Ti$_{0.84}$Sn$_{0.16}$)O$_3$ shows a quite uniform grey intensity distribution feature, and no bright contrast regions can be observed. These structural differences between the ferroelectric and relaxor compounds were also verified in the images from other crystal zone axes in the samples, and the same results were obtained.

Our dark field images not only show these distinct nanoregions directly [Figs. 1(a) and 1(b)], they also show that these nanoregions are embedded in a matrix with a structure which is likewise related to the diffuse electron scattering. As shown in Fig. 1(c) for the normal ferroelectric Ba(Ti$_{0.84}$Sn$_{0.16}$)O$_3$, the intensity of the diffuse scattering (see inset) is about the same
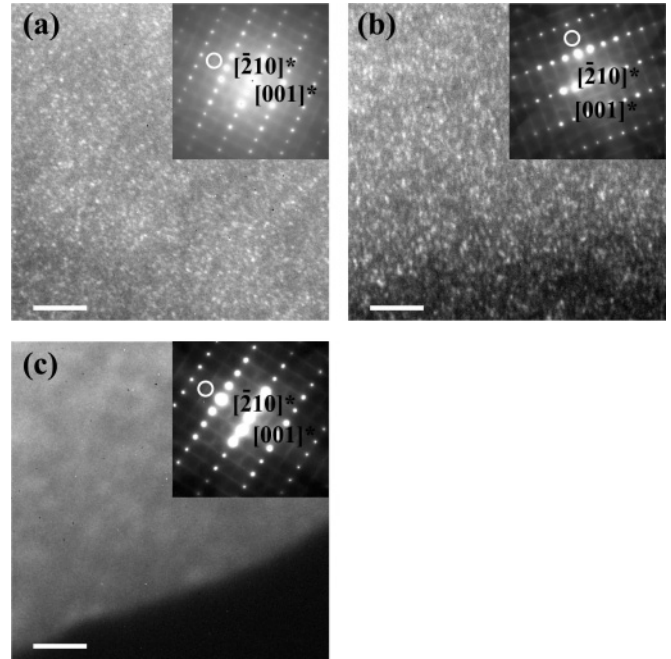

FIG. 1. Dark field images of (a) Ba(Ti$_{0.8}$Sn$_{0.2}$)O$_3$, (b) Ba(Ti$_{0.75}$Sn$_{0.25}$)O$_3$, and (c) Ba(Ti$_{0.84}$Sn$_{0.16}$)O$_3$ taken from the ⟨120⟩ zone axis. The scale bars are 10 nm. The selected area diffraction patterns are given in the insets, and the white circles indicate the location of the objective aperture used for dark field imaging. Nanosize static polar clusters with bright contrast are clearly seen in (a) and (b), while no such contrast feature is observed in (c).

as in the relaxors. The grey intensity indicates that there are atom correlations, but no distinct nanoregions occur. These results can be explained as follows. In all three compounds, we have the atom correlations present, which give rise to the diffuse intensity in diffraction. In the relaxor-forming compounds, discrete and well-defined nanoregions occur, and their lifetime is large compared to the exposure time of the micrographs (about 7 s). In between these discrete and static nanoregions, the matrix is also characterized by local ordered atom correlations, but these are too small and fuzzy to give any discrete contrast. It is also possible that these correlations are forming and decaying too rapidly to show up in the images. In the case of the normal ferroelectric compound, the lifetime of possibly forming polar regions in the paraelectric phase is so small that, during the exposure time, the contrast is averaged out. Since there is no indication of even a grainy structure, we can also expect that the extension of the fluctuations is small so that, in projection (with the contrast overlapping), no net contrast but the uniform intensity background can be observed. We point out that large fluctuations (precursor polarization clusters) are expected in the vicinity of any continuous (or weakly first order) phase transition. They were indeed observed in pure BaTiO$_3$ by means of photon correlation spectroscopy[31] and by the picosecond soft x-ray laser speckle technique.[32,33] The fluctuation lifetime was found to be of the order of 10–100 ps.[33] In contrast to the normal ferroelectric compound, the relaxor-forming compounds are characterized above T_f by polar nanoregions of long lifetime, which allows us to consider them as stable entities. A possible
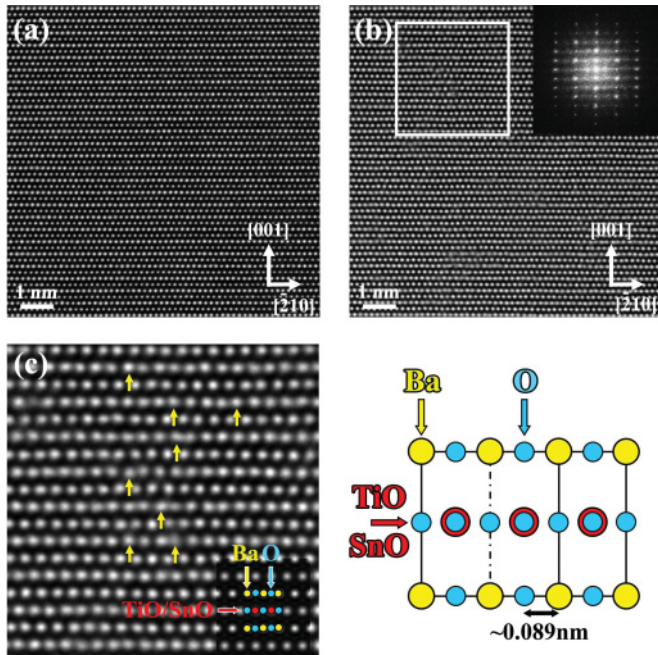
FIG. 2. (Color online) HRTEM images of (a) $Ba(Ti_{0.84}Sn_{0.16})O_3$ and (b) $Ba(Ti_{0.75}Sn_{0.25})O_3$ viewed from $\langle 120 \rangle$ zone axis. The framed area in (b) is enlarged and displayed in (c). The projection of the crystal structure as well as the image simulation result is superimposed on the image. The yellow/light gray arrows indicate, as examples, local displacements of the B-site atoms.

mechanism for their formation in disordered relaxor-forming crystals has been discussed in Ref. 34.

The above results are also corroborated by direct insights into their atomic structures by employing the quantitative high-resolution transmission electron microscopy technique. The atomic-resolution images of the ferroelectric-forming $Ba(Ti_{0.84}Sn_{0.16})O_3$ and the relaxor-forming $Ba(Ti_{0.75}Sn_{0.25})O_3$ are shown in Figs. 2(a) and 2(b) as examples. The viewing direction of these images is along the crystallographic $\langle 120 \rangle$ direction. In these images, the Ba and Ti/Sn atoms appear as bright contrast on the dark background. The oxygen atoms cannot be resolved here since, due to the low nuclear charge, their contrast is too weak. Also, the separation between the Ti/Sn and O atoms viewing in the $\langle 120 \rangle$ direction is about 0.089 nm, and this is close to the resolution limit of our microscope. The above image features are fully reproduced by image simulation (see the Supplemental Material[25]), and this provides the basis for interpreting the structures from these images. The essential differences between the ferroelectric and relaxor compounds are clearly revealed in Figs. 2(a) and 2(b) on an atomic scale. While the uniform atomic contrast of Fig. 2(a) indicates a good alignment of the atoms except for some strained areas, the locally varying atomic contrast in Fig. 2(b) shows a short-range ordering feature of the Ti/Sn positions (readily visible regarding the image at gracing angle). This short-range order feature can be seen more clearly in Fig. 2(c), which is magnified from the framed area in Fig. 2(b). The yellow/light gray arrows in Fig. 2(c) indicate the Ti/Sn atom columns which are displaced significantly relative to each other as a guide of eye. It should be noted here that the individual contrast maxima, since the sample

is imaged in $\langle 120 \rangle$ zone axis, are the result of the dynamic electron propagation along atomic columns of 5 to 10 nm long in the incident beam direction. As a consequence, the atomic distortions are averaged out, and only for the cases where the averaging along the thickness of the specimen is resulting accidentally in an appreciable net deviation from the average, an effect of local atomic displacements can be seen. Nonetheless, the fact that we see such deviations from the regular pattern in Figs. 2(b) and 2(c) and not in Fig. 2(a) provides us with solid evidence for the local variation of polarizations in the relaxor-forming compounds.

The spatial distribution of the local atom displacements provides invaluable information of the PNRs' atomic structures. For this, we employ a standard peak finding algorithm based on fitting two-dimensional Gaussian functions to the intensity maxima.[26] Based on these data, the lateral displacements of individual B-site atom columns are calculated according to

$$\mathbf{u}_{ij} = \mathbf{r}_{ij} - \bar{\mathbf{r}}_{ij}, \tag{1}$$

where ij are indices characterizing a particular atomic column in the image; $\mathbf{r}_{ij}$ and $\bar{\mathbf{r}}_{ij}$ denote the measured and the averaged crystal atom-column position, respectively. The calculated results are displayed in Fig. 3, where local displacements of individual Ti/Sn-atom columns are shown as vectors for (a) $Ba(Ti_{0.84}Sn_{0.16})O_3$, (b) $Ba(Ti_{0.8}Sn_{0.2})O_3$, and (c) $Ba(Ti_{0.75}Sn_{0.25})O_3$, respectively. The magnitudes of the displacements are also shown as contour maps. For $Ba(Ti_{0.84}Sn_{0.16})O_3$ [Fig. 3(a)], the spatial distribution of the displacements is essentially uniform, and their standard deviation is about 0.006 nm. This value is rather small and is comparable to the measurement error ($\sim$0.005 nm, see Ref. 27 for details), suggesting a highly symmetrical structure with
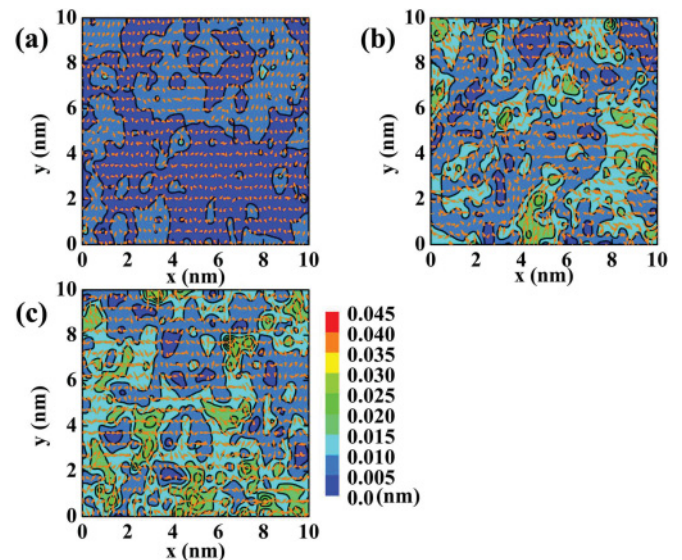

FIG. 3. (Color online) Displacements maps represented by arrows of (a) $Ba(Ti_{0.84}Sn_{0.16})O_3$, (b) $Ba(Ti_{0.8}Sn_{0.2})O_3$, and (c) $Ba(Ti_{0.75}Sn_{0.25})O_3$. The magnitudes of the displacements are presented by contours, providing evidence for static polar nanoregions in (b) and (c). The static polar clusters are formed in the vicinity of local displacement maxima, and the standard deviations of local displacements are 0.012 and 0.014 nm, respectively (see text for details).

very small local polarization fluctuations. However, as we've discussed above, the PNRs should be evenly distributed in the ferroelectrics, but they are not observed here. A viable explanation could be as follows: the PNRs are indeed present throughout the crystal, but they are dynamically flipping by thermal activations at a time scale of $\sim 10^{-12}$ s. Since the acquisition time ($\sim 10^0$ s) in our experiment is much longer than the PNRs' dynamics, their polarizations are time averaged, and a structure without local static distortions is observed. We also note that there are some locally distorted regions present, but they may be the result of a local nonuniform distribution of the Sn atoms.

A substantially different result is obtained for the two relaxor-forming compounds [Figs. 3(b) and 3(c)]. The contour maps depict a complex arrangement of the regions with aggregated large atom displacements. The standard deviations of the atom displacements of $Ba(Ti_{0.8}Sn_{0.2})O_3$ and $Ba(Ti_{0.75}Sn_{0.25})O_3$ are 0.012 and 0.014 nm, respectively. These values are much larger than that of the ferroelectric $Ba(Ti_{0.84}Sn_{0.16})O_3$. Further analysis shows that the atomic displacements within these regions are spatially correlated up to several unit cells (see the Supplemental Material[25]), and their typical lateral size extends from subnanometer size up to about 2 nm, which matches the dimension of the bright polar regions observed in the dark field images very well. Considering their spatial correlations, we suggest that these areas with large correlated atom displacements are indeed the PNRs. It should be emphasized that the PNRs observed here may have a different origin from their dynamic counterparts. These PNRs are truly static since they're essentially captured in a timescale (about 10^0 s), much longer than the dynamic PNRs' characteristic time ($\sim 10^{-12}$ s). Otherwise, a time-averaged structure will be observed. Besides the static PNRs with large local displacements, there are also regions where the net displacements are very small. These regions in between the static PNRs can either be the result of a static behavior of the truly nonpolar matrix or of the time-averaging of the continuously flipping dynamic PNRs.

Our experimental results clearly reveal the structure differences between the ferroelectric and the relaxors in the lead-free $Ba(Ti_{1-x}Sn_x)O_3$ system on an atomic scale. This understanding helps to explain different experimental results in many aspects. As was shown in our experiment, the structural disorder, e.g. local atomic distortions caused by the Sn substitutions, is very limited, and the structure is very similar to the paraelectric cubic $BaTiO_3$ for the ferroelectric solid solution $Ba(Ti_{0.84}Sn_{0.16})O_3$. Therefore, a long-range ferroelectric order state under the constraint of local strain field is expected to form upon cooling down. Indeed, a much complex domain structure with size ranging from several hundred square nanometers to square submicrometers instead of a well-defined ferroelectric domain structure was reported.[24,35] This structure with mesoscopic complexity was considered to be an intermediate state between ferroelectrics and relaxors rather than a normal ferroelectric state.[24] Nonetheless, the structure is still ferroelectric on the nanoscale and atomic scale. The structure is, however, much more complex for the relaxors, where local quenched static PNRs are formed. These static PNRs can also give rise to the same diffuse scattering features as the dynamic PNRs. As a result, the electron diffraction diffuse scatterings remain essentially identical irrespective of the composition and the structure.[9,22,23] Also, the size of these static PNRs is too small to be probed by the piezoresponse force microscopy method, and as a result, their piezoactivity could not be observed.[24]

The possible mechanism for the static PNRs formation can be the result of local composition fluctuations, which act as sites to quench local polar structures and where a local phase transition takes place.[34] It may also be suggested that some PNRs are already frozen at high temperature due to their much larger size. However, the size of the static PNRs (~ 2 nm) seems to be too small. In spite of the mechanism, the presence of static PNRs in the relaxors at a temperature range far above T_f is unambiguously evident from our experiment. According to the spherical random bond-random field theory,[36] the formation of a long-range ordered ferroelectric state or a relaxor state is determined by the relative strength of the dipole interaction and the random field. In the presence of a strong random field, the long-range ordered ferroelectric state is prevented from forming. This is similar for the lead-free relaxor $Ba(Ti_{1-x}Sn_x)O_3$, where static polar structures are formed, and the material is broken into fragments without long-range order. The static polar structures could also introduce local static internal electric fields and impose constraints on the motions of dynamic PNRs. As a result, the dynamics of the dynamic PNRs as well as the dielectric response of the whole crystal are also affected. It is worth pointing out that the static PNRs are not only the characteristic of the lead-free $BaTiO_3$-based relaxors, but also of the lead-containing relaxors. Recent experiments by using switching spectroscopy piezoresponse force microscopy reported the presence of a mesoscopic static PNRs structure in PMN-10PT.[37] Using neutron scattering techniques, it was found in PMN that static PNRs with at least 2 ns lifetime are formed below the Burns temperature.[38] These static PNRs are suggested to be pinned by local chemical order inside the chemically ordered regions.[20]

IV. CONCLUSIONS

In conclusion, the nano and atomic structures of ferroelectric- and relaxor-forming $Ba(Ti_{1-x}Sn_x)O_3$ compounds were investigated by dark field imaging and aberration-corrected high-resolution electron microscopy. Static PNRs with local large atomic displacements were revealed for the relaxor-forming compounds above the freezing temperature for the first time, while a structure with regular lattice was found for the ferroelectric compound. These experiment results suggest that the relaxor behaviors in the lead-free $Ba(Ti_{1-x}Sn_x)O_3$ system may be closely related to the formation of static polar nanoregions. Finally, we want to point out that combining the dark field imaging and the imaging of local atomic displacements and thus investigating the structure of PNRs provide a basis for studying the relaxor materials and their mechanisms.

---

[*]Corresponding author: jzhu@mail.tsinghua.edu.cn; Dr. Jing Zhu, Schl. of Mat. Sci. + Eng., Tsinghua Univ., Beijing 100084, China.

[1]K. Uchino, Ferroelectrics **151**, 321 (1994).

[2]J. Cieminski and H. Beige, J. Phys. D: Appl. Phys. **24**, 1182 (1991).

[3]C. Lei, A. A. Bokov, and Z. G. Ye, J. Appl. Phys. **101**, 084105 (2007).

[4]A. Simon, J. Ravez, and M. Maglione, J. Phys.: Condens. Matter **16**, 963 (2004).

[5]C. Ménoret, J. M. Kiat, B. Dkhil, M. Dunlop, H. Dammak, and O. Hernandez, Phys. Rev. B **65**, 224104 (2002).

[6]Y. Zhi, A. Chen, R. Guo, and A. S. Bhalla, J. Appl. Phys. **92**, 1489 (2002).

[7]Ang Chen, Yu Zhi, and Jing Zhi, Phys. Rev. B **61**, 957 (2000).

[8]N. Yasuda, H. Ohwa, and S. Asano, Jpn. J. Appl. Phys., Part 1 **35**, 5099 (1996).

[9]Y. Liu, R. L. Withers, B. Nguyen, and K. Elliott, Appl. Phys. Lett. **91**, 152907 (2007).

[10]X. Y. Wei, Y. J. Feng, and X. Yao, Appl. Phys. Lett. **83**, 2031 (2003).

[11]L. E. Cross, Ferroelectrics **76**, 241 (1987).

[12]G. A. Samara, J. Phys. Condens. Matter **15**, R367 (2003).

[13]L. E. Cross, Ferroelectrics **151**, 305 (1994).

[14]C. A. Randall and A. S. Bhalla, Jpn. J. Appl. Phys. **29**, 327 (1990).

[15]S. Tinte, B. P. Burton, E. Cockayne, and U. V. Waghmare, Phys. Rev. Lett. **97**, 137601 (2006).

[16]B. P. Burton, E. Cockayne, and U. V. Waghmare, Phys. Rev. B **72**, 064113 (2005).

[17]H. Z. Jin, J. Zhu, S. Miao, X. W. Zhang, and Z. Y. Cheng, J. Appl. Phys. **89**, 5048 (2001).

[18]S. Miao, X. W. Zhang, and J. Zhu, J. Am. Ceram. Soc. **84**, 2091 (2001).

[19]N. Lu and J. Zhu, J. Appl. Phys. **104**, 034109 (2008).

[20]S. Vakhrushev, *Abstract Book of the 11th European Meeting on Ferroelectricity* (Bled, Slovenia, 2007), p. 219.

[21]G. Y. Xu, G. Shirane, J. R. D. Copley, and P. M. Gehring, Phys. Rev. B **69**, 064112 (2004).

[22]Y. Liu, R. L. Withers, X. Y. Wei, and J. D. Fitz Gerald, J. Solid State Chem. **180**, 858 (2007).

[23]S. Miao, J. Pokorny, U. M. Pasha, O. P. Thakur, D. C. Sinclair, and I. M. Reaney, J. Appl. Phys. **106**, 114111 (2009).

[24]V. V. Shvartsman, W. Kleemann, J. Dec, Z. K. Xu, and S. G. Lu, J. Appl. Phys. **99**, 124111 (2006).

[25]See Supplemental Material at http://link.aps.org/supplemental/10.1103/PhysRevB.85.014118 for details.

[26]C. L. Jia, M. Lentzen, and K. Urban, Science **299**, 870 (2003).

[27]C. L. Jia, S. B. Mi, K. Urban, I. Vrejoiu, M. Alexe, and D. Hesse, Nat. Mater. **7**, 57 (2008).

[28]C. L. Jia, M. Lentzen, and K. Urban, Microsc. Microanal. **10**, 174 (2004).

[29]M. A. O'Keefe and R. Kilaas, Scan Microsc. Suppl. **2**, 225 (1988).

[30]A. Bokov and Z. G. Ye, J. Mater. Sci. **41**, 31 (2006).

[31]R. Yan, Z. Guo, R. Tai, H. Xu, X. Zhao, D. Lin, X. Li, and H. Luo, Appl. Phys. Lett. **93**, 192908 (2004).

[32]R. Z. Tai, K. Namikawa, A. Sawada, M. Kishimoto, M. Tanaka, P. Lu, K. Nagashima, H. Maruyama, and M. Ando, Phys. Rev. Lett. **93**, 087601 (2004).

[33]K. Namikawa, M. Kishimoto, K. Nasu, E. Matsushita, R. Z. Tai, K. Sukegawa, H. Yamatani, H. Hasegawa, M. Nishikino, M. Tanaka, and K. Nagashima, Phys. Rev. Lett. **103**, 197401 (2009).

[34]A. A. Bokov, Phys. Solid Stat. **36**, 19 (1994).

[35]S. G. Lu, Z. K. Xu, and H. Chen, Appl. Phys. Lett. **85**, 5319 (2004).

[36]R. Pirc and R. Blinc, Phys. Rev. B **60**, 13470 (1999).

[37]A. A. Bokov, B. J. Rodriguez, X. Zhao, J. H. Ko, S. Jesse, X. Long, W. Qu, T. H. Kim, J. D. Budai, A. N. Morozovska, S. Kojima, X. Tan, S. V. Kalinin, and Z. G. Ye, Z. Kristallogr. **226**, 99 (2011).

[38]P. M. Gehring, H. Hiraka, C. Stock, S. H. Lee, W. Chen, Z. G. Ye, S. B. Vakhrushev, and Z. Chowdhuri, Phys. Rev. B **79**, 224109 (2009).